IJST (2014) 38A2: 145-158
Iranian Journal of Science & Technology

http://ijsts.shirazu.ac.ir

Geochemical behavior of Mo and precious metals during supergene enrichment in the SarCheshmeh porphyry Cu deposit, Iran

B. Shafiei

Department of Geology, Faculty of Sciences, Golestan University, Gorgan, Iran
E-mail: behnam.shafiei@gmail.com

Abstract

Supergene oxidation-leaching and secondary sulfide enrichment in the SarCheshmeh porphyry Cu-Mo deposit generated a supergene profile to depths of 20 to 80 meters with oxide ore reserve about 22 Mt. @1.08% Cu and sulfides ore reserve~106Mt.@1.27% Cu. Geochemical distribution and behavior of trace metals associated with Cu namely Mo, Au, and Ag in the supergene profile of the SarCheshmeh were poorly understood and documented. To this aim, using a relatively large geochemical dataset along with theoretical data allowed distribution of the metals in the supergene profile to be clarified, and to be discussed behavior of Mo, Au, and Ag during supergene enrichment process of the SarCheshmeh deposit. Constraints on distribution and mobility of trace metals in the supergene environment of the SarCheshmeh deposit indicated that Au strongly enriched in the chalcocite zone. During supergene oxidation and leaching, Mo significantly remained in the leached cap, whereas Ag tends to be partially fixed in oxidized ore zone and locally enriched in chalcocite zone. Observed difference in the geochemical mobility of the metals is function of change in pH, Eh and metal-transporting capacity of supergene solutions. Under high acidic condition of supergene solutions which corresponded to oxidation of pyrite-rich primary ores (e.g., sericitized samples), mobility of Mo is greatly restricted with formation of ferrimolybdite in leached zone which has prevented supergene sulfide enrichment of Mo. This caused local enrichment of Mo (average~0.020 %) associated with Fe-oxides in leached ores which are supported by moderately positive correlation between Mo and Fe_2O_3 (r=+0.75) in such ores. Under such conditions, Au is strongly mobilized possibly as auric-chloride complexes rather than thiosulfates, and appreciably enriched in chalcocite zone. This is consistent with the low neutralizing capacity of the pyrite-rich primary ores along supergene solutions pathway and also semi-arid climate of the SarCheshmeh region. Unlike Au, soluble Ag in high acidic supergene solutions tends to be locally fixed in oxidized zone and to some extend enriched in chalcocite zone. This could relate to rapid decomposition of the halide complexes, consequently leaving silver as Ag-halide minerals, arjento-jarosite and/or native silver in oxidized ores without gold. This is supported by the negative correlation between Ag and Au values in oxidized ores (r= -0.28). Partial enrichment of Mo in chalcocite zone indicate that pH of supergene solutions derived from oxidation of pyrite-poor ores (biotitized ores) could remain above the stability field of ferrimolybdite (pH=5); this led to mobilization of Mo and locally enrichment of Mo in chalcocite zone. Where these conditions apply there may be local retention of Au in the form of native gold within leached ores.

Keywords*:* Trace metals; supergene; Cu porphyry; SarCheshmeh; Iran

1. Introduction

Supergene enrichment in porphyry Cu deposits is an economically weathering process that concentrates metals within the supergene profile commonly two or three times the hypogene tenor (Sillitoe, 2005; Sillitoe, 2009). Consequently, the presence of the supergene profiles has a major economic impact on mining of these deposits. During supergene process, some metals extensively leach from weathering front and will be enriched towards the base of the supergene profile. In addition, several metals remain inleached cap and will be relatively enriched therein due to leaching of the other constituents from the weathering front. Factors that appear to control metals distribution and their mobility during supergene oxidation process (Boyle, 1968; Boyle, 1978; Webster and Mann, 1984; Stoffregen, 1986; LeAnderson et al., 1987; Benedetti and Boulegue, 1991; Greffie et al., 1996; Sillitoe, 2005; Sillitoe, 2009) include sulfide and alteration mineralogy of primary ores, climatic influences, geomorphology, hydrologic conditions and groundwater composition. Different combinations of these factors generally produce different results. The SarCheshmeh porphyry copper deposit containing~1700 Mt of total ore reserves (~850 Mt past production+828 Mt

Received: 1 August 2012 / Accepted: 5 April 2014

remained reserve) with an average of 0.65 % Cu, 0.02 % Mo (unpublished new data of SarCheshmeh Copper Complex, 2012), 0.06 g/t Au, and 1.22 g/t Ag (Shafiei, 2010) is presently the largest producer of Cu, Mo, and Au in Iran owned by National Iranian Copper Industries Company (NICICo). Significant tonnage of Cu as oxide (~22 Mt.@1.08% Cu; unpublished report of Anaconda-Iran Inc., 1974) and secondary sulfides (~106 Mt.@1.27% Cu; unpublished new data of SarCheshmeh Copper Complex, 2012) is contained in oxidized zone and chalcocite zone of supergene profile in the SarCheshmeh deposit. It is an important economic feature of the SarCheshmeh deposit. Hypogene and supergene Cu mineralization and also hydrothermal evolution in the SarCheshmeh deposit is well studied and described (Waterman and Hamilton, 1975; Etminan, 1981; Haynes and Ghorashizadeh, 1978; Shahabpour, 1982; Shahabpour and Kramers, 1987; Shahabpour, 1991; Shahabpour, 2000), but distribution of the trace metals namely Mo, Au, and Ag and their mobility in supergene profile of the SarCheshmeh deposit are still poorly documented. The current study is governed for better understanding of the trace metals distribution and their behavior in the supergene profile of the porphyry Cu deposits. To this aim, using a relatively large geochemical dataset along with theoretical data allowed distribution of the metals in the supergene profile to be clarified, and behavior of the trace metals during supergene Cu enrichment process of the SarCheshmeh deposit to be discussed.

2.Geological background

2.1. Ore deposit geology

Regionally, the SarCheshmeh deposit is located in the southern segment of central Iranian volcano-plutonic belt (Cenozoic magmatic arc; Fig. 1a). The geological environment of the SarCheshmeh deposit is similar to many porphyry copper deposits in the Chilean Andes and western Cordillera of North America which is principally composed of a folded and faulted Tertiary igneous-sedimentary complex (Nedimovic, 1973). This complex mainly consists of Eocene volcanic and sedimentary successions, Oligo-Miocene intrusions and dikes, Plio-Pleistocene ignimbrites, tuff-breccias and a volcanic center. Although the vicinity of the deposit consists of rough mountainous topography with elevations ranging from 3280 to 2500 m, because of rapid erosion of the relatively soft, altered rocks a broad basin with dune-bedded morphology has been formed in the SarCheshmeh deposit. At the deposit-scale, the orebody is ellipsoid-shaped, about 2300 meters long by 1200 meters wide (unpublished new data of SarCheshmeh Copper Complex., 2012), and is centered in a granodiorite which is called SarCheshmeh porphyry stock (SCP: Shahabpour and Kramers, 1987; Fig.1b). Ore-hosting stock was emplaced at 13.6±0.1 Ma (U-Pb on apatite; McInnes et al., 2005) within Eocene fine-grained porphyritic andesites (Unpublished report of Selection Trust Ltd., 1970). The core area of the deposit (ore-hosting stock; SCP) appears to have been intruded by a fine-grained porphyritic plug at about 12.1 Ma (Rb-Sr on biotite; Shahabpour, 1982), which is called late fine-grained porphyry (LFP: Shahabpour and Kramers, 1987; Fig.1b). Finally, a series of intra- to post-mineralization dikes (i.e., EHP: early hornblende porphyry; LHP: late hornblende porphyry; FP: feldspar porphyry; BP: biotite porphyry) with different composition and age (from 8.3±0.4Ma to 3.4±1Ma; Haynes and Ghorashizadeh, 1978; McInnes et al., 2005) intruded the porphyries and andesitic wall-rock (Fig.1b).

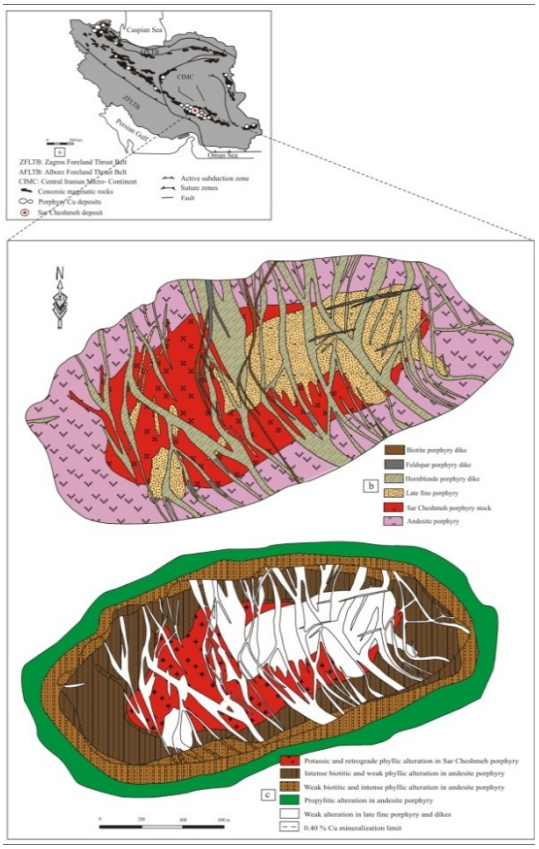

Fig. 1(a). Map showing the location of the SarCheshmeh deposit in central Iranian volcano- plutonic belt (simplified from Shafiei et al. 2009). **(b).** General distribution of main rock types in the SarCheshmeh deposit within 0.40% Cu cutoff at 2400 meters elevation (modified from Waterman and Hamilton, 1975). **(c).**Hypogene alteration pattern in the SarCheshmeh deposit within the 0.40% Cu cutoff at 2400 meters elevation (modified from Waterman and Hamilton, 1975)

2.2. Hypogene alteration and mineralization

Hydrothermal alteration and mineralization in the SarCheshmeh deposit occurred in both the SCP stock and the andesitic wall-rock (Waterman and Hamilton, 1975; Haynes and Ghorashizadeh, 1978; Etminan; 1981; Shahabpour, 1982; Shahabpour and Kramers, 1987; Shahabpour, 1991; Shahabpour, 2000) about 12.9 Ma (U-Pb on apatite; McInnes et al., 2005). LFP and EHP dikes are altered and weakly mineralized, others are barren (Fig. 1c). The main types of hypogene pervasive alteration are distinguished which are arranged with respect to their spatial distribution from the center of the deposit (SCP stock) to the outside (andesitic wall-rock) including potassic (as well as K-feldspar in SCP stock and biotitic in andesitic wall-rock), potassic affected by phyllic, strong phyllic±argillic, and propylitic alteration (Fig. 1c). Hypogene mineralization occurred in three main stages namely the early, transitional, and the late stages as cross-cutting veinlets (stock-work) and dissemination. The predominant sulfides in the hypogene zone are pyrite, chalcopyrite, and molybdenite which are associated with quartz veinlets. Constraints on hypogene distribution of Mo and precious metals (Au and Ag) in the SarCheshmeh porphyry copper deposit indicated that much of the metals tend to be concentrated within the Cu-rich potassic and strongly phyllic alteration zones (Shafiei and Shahabpour, 2012). The metals grade decreases towards the center of the stock, which is apparent by low-grade core (Cu=0.08-0.36%, Mo=0.001%-0.009%, Au=0.010-0.032 g/t, Ag=0.24-1.40 g/t; Shafiei and Shahabpour, 2012). The gradual increase in metal concentrations from weak potassic alteration to strong potassic (Cu=0.52%-1.48%,Mo=0.009%-0.084%, Au=0.022-0.098 g/t, Ag= 0.42 - 2.40 g/t; Shafiei and Shahabpour,2012) and phyllic zones (Cu=0.74%-1.63%, Mo=0.002%-0.196%, Au=0.017-0.120 g/t, Ag=0.51-5.50 g/t; Shafiei and Shahabpour, 2012) is observed that could relate to cumulative effects of the early to the late stages of alteration and mineralization which is increased vein density and metal deposition (Shafiei and Shahabpour, 2012). Generally, the propylitized andesitic wall-rock indicated the lowest grades of the metals like to the low-grade core of the deposit (Cu=0.19%-0.34%, Mo=0.001%-0.016%, Au=0.016-0.031g/t, Ag=0.48-1.25 g/t; Shafiei and Shahabpour, 2012). Relationship between hypogene grades of the metals in different ore types indicated that precious metals and Cu positively correlate over a wide range of values, indicating a spatial and temporal association of precious metals with Cu sulfides. In contrast, the sympathetic relationship of Mo with Cu and precious metals is only present in low-grade ores which are deposited in weak potassic alteration zone. This suggested contemporaneous deposition of minor Mo with Cu and precious metals during the early stage of mineralization. In the transitional stage of mineralization, a significant portion of Mo deposition occurred independent of Cu and precious metals which is supported by the negative correlation between Mo and Cu (also with precious metals) in silicified ores. In the late stage of mineralization, where the highest values of the metals is occurred with sericitization, differences in distribution of the metals are significant, that could be attributed to the heterogeneous distribution of Mo, Cu and precious metals during the evolution of the porphyry system (Shafiei and Shahabpour, 2012). Study on sulfide zoning in hypogene ores indicated that hypogene Cu grade increased in andesitic wall-rock and SCP stock associated with increasing of the chalcopyrite-pyrite ratio. Excluding the sericitized outer fringe zone it is clear that within the internal zone of sericitic alteration the chalcopyrite-pyrite ratio is higher in SCP stock than in the andesitic wall-rock. Also, the chalcopyrite-pyrite ratio is higher in weakly altered SCP stock and biotitized andesitic wall-rock than sericitized rocks. In propylitized andesitic wall-rock, where pyritic halo is well-developed, chalcopyrite-pyrite ratio is higher than other zones (unpublished report of Anaconda-Iran Inc., 1974; Waterman and Hamilton, 1975).

2.3. Supergene profile

Exhumation of the SarCheshmeh porphyry complex in 5.20 Ma (McInnes et al., 2005) was followed by recent erosion and oxidation-leaching of the ores. The semi-arid weathering produced a supergene weathering profile to depths of several ten meters comprising leached cap, oxidized zone, and chalcocite zone (unpublished report of Selection Trust Ltd., 1970; Waterman and Hamilton, 1975; Figs. 2a and 3a). Leached cap in the SarCheshmeh deposit is developed as a surface layer of iron oxides averaging 26 meters in thickness overlying the oxide and chalcocite zones (Waterman and Hamilton, 1975). Leached cap in the SarCheshmeh deposit typified by the presence of oxidized Fe minerals group (e.g., goethite, hematite, and jarosite) with colloform texture and also residual pockets of primary Cu-Fe sulfides (box-work texture) which have been oxidized (Fig. 2).

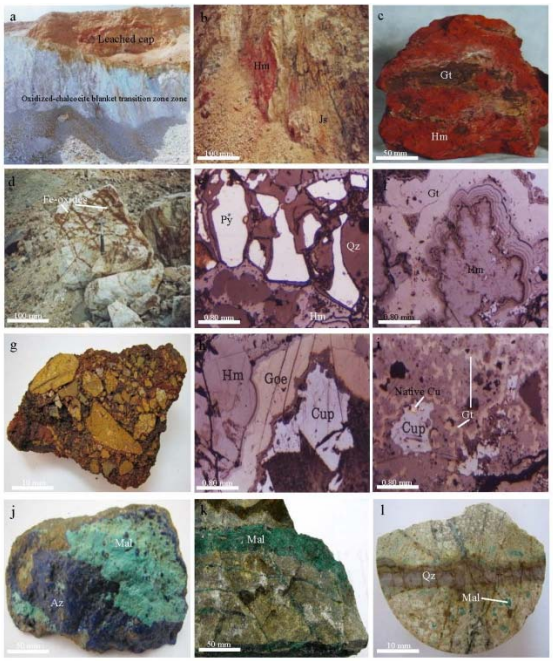

Fig. 2. Photographs and microphotographs of leached cap, oxidized ore zone and related mineralization; **a.** A view of the northern wall of the open pit at the SarCheshmeh mine; leached cap is hematitic and goethitic, oxidized-chalcocite transitional ore zone contains abundant Fe and Cu sulfates and secondary Cu sulfides (chalcocite). **b.** hematitic and jarositic leached cap in the southern wall of the open pit. Grayish black veins are Cu-Fe sulfides which converted to Cu and Fe oxides. **c.** Hand specimen of the leached ore composed of hematite (Hm), goethite (Gt), and jarosite (Js). **d.** Oxidation of quartz-sulfide stringers in a large block of leached argillic ores. **e.** Microphotograph showing immature oxidation of pyrite in a quartz-pyrite veinlet of a leached ore. **f.** Closed-up image of coloform texture of hematite and goethite in the leached ores. **g.** Hand specimen of an unroofing breccia (fragmentite) cemented by a matrix of iron oxides and hydroxides and rock fragments. **h.** Microphotograph of cuprite (Cup)- hematite-goethite assemblage in a sample from transition zone. **i.** Microphotograph showing paragenesis of cuprite and native Cu in oxidized ore sample. **j.** Crustification of malachite and azurite on the oxidized ore sample. **k.** Malachite replacing Cu-sulfide stringers in andesitic wall-rock sample. **l.** Hand specimen of malachite within the argillitic plagioclase phenocrysts of the SarCheshmeh porphyry stock

Supergene oxidation and leaching process in the SarCheshmeh deposit has strongly occurred inside the central alteration zones (potassic and phyllic), whereas the peripheral alteration zone, the propylitic or unaltered andesitic wall-rock shows little or no supergene leaching of sulfides. The thickness of leached capping is estimated variable, being as much as 84 m under the higher ground (hills), while in the creeks and valleys it is thin, only a few meters thick or may be absent due to erosion (unpublished report of Selection Trust Ltd., 1970; Waterman and Hamilton, 1975). The mineralogy of iron oxides in the leached capping could be controlled by sulfide mineralogy of primary ores. Over pyrite-rich ores especially in sericitizedandesites and also pyritic halo, leached cap characterized by the abundance of hematite and also jarosite. In contrast, goethite is predominant Fe-oxides in leached caps that developed over the hypogene pyrite-poor ores such as biotitizedandesites and potassicSarCheshmeh porphyry stock. The contact zone between the leached capping and oxidized zone is gradational. In some drill cores a transitional zone of mixed leached and oxide ores is present with maximum thickness about 84 m under the higher ground (unpublished report of Selection Trust Ltd., 1970). The most important of the oxide mineralization appears to have been formed in transitional zone and near the top of the supergene chalcocite zone. Oxide mineralization consists mainly of copper carbonates, malachite and azurite; also minor amount of cuprite, native copper, turquoise, delafossit, copper pitch, cupriferous sericite, and copper clays along with Fe-oxides is reported (unpublished report of Selection Trust Ltd., 1970; Shahabpour, 1982; Shahabpour, 1991; SalariRad et al., 1999; Fig. 2). Further, non-significant oxide mineralization occurred overlying hypogene sulfides where chalcopyrite-pyrite ratio was high and hypogene sulfide minerals were oxidized in-situ to carbonates. There is a well-developed supergene chalcocite zone with significant Cu tonnage in the lower parts of the supergene profile (Fig. 3). Drilling has shown that the thickness of the chalcocite zone varies greatly; its development depends on many factors such as rate of erosion, surface relief, and presence of dyke. The chalcocite zone shows maximum thickness (up to 150 m thickness) under the ridges and over hypogene high grade ores, especially where phyllic alteration is well developed (unpublished report of Selection Trust Ltd., 1970; unpublished report of Anaconda-Iran Inc., 1974). It is thin under the main creeks, valleys, and on the edges of the deposit, where pyritic halo is developed on propylitic zone; less than 20 m thickness (unpublished report of Selection Trust Ltd., 1970; unpublished report of Anaconda-Iran Inc., 1974). The average thickness of supergene chalcocite zone is estimated about 37 meters (Waterman and Hamilton, 1975). The bottom of the chalcocite zone is often gradational, and normally shows irregularities due to local channeling of the Cu-bearing groundwater solutions between dykes and possibly along the faults and fractures. Dikes which contained significant minor hypogene sulfides were erratically enriched to supergene ore. Enrichment is more pronounced adjacent to dike- porphyry contacts, often structural zones that facilitated supergene solution percolation. Narrow dikes may show significant enrichment; in the central portions of thick dikes chalcocite zone is thin and poorly developed. Microscopic observations indicate that discrete grains of chalcocite can be seen where the

chalcopyrite and pyrite in the upper parts of the chalcocite zone have been completely replaced; but, more typically, the chalcocite forms replacement rims and veinlets in the chalcopyrite grains, and to a lesser extent, in the pyrites; especially in lower parts of the chalcocite zone (Fig. 3). Bornite, covellite, and digenite are sporadically present in minor importance near the bottom of the chalcocite zone. Alteration associated with supergene enriched ores consists of sericite and kaolinite overlying zones of strong hypogene altered rocks and predominately clay minerals over weakly altered ore zones.

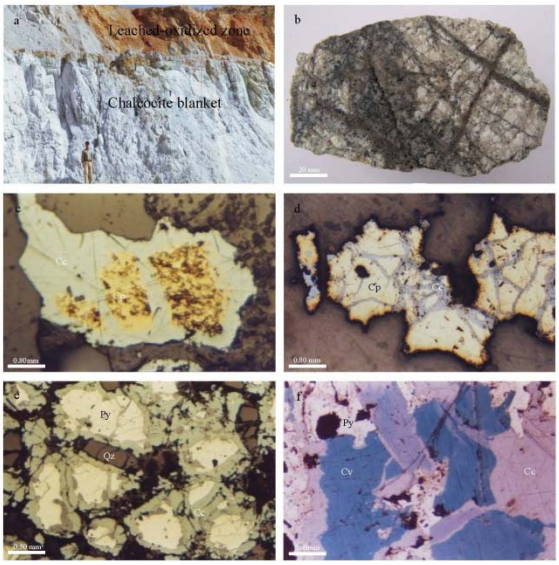

Fig. 3. Photographs and microphotographs of the supergene chalcocite zone and mode of related mineralization; a. A view of chalcocite zone developed under the leached-oxidized ore zone in northeastern wall of the open pit. b. Hand specimen of the SarCheshmeh porphyry stock within the chalcocite zone containing cross-cutting thin and thick quartz-chalcocite veinlets and dissemination chalcocite (black dots). c-d. Closed-up image showing partly replacement of chalcopyrite (Cp) by chalcocite in the SarCheshmeh porphyry stock ore sample. e. Closed-up image of disseminated pyrites (Py) replaced by chalcocite in a sample of andesitic wall-rock ores. f. Closed-up image of covelite (Cv) and chalcocite replacing pyrite in the SarCheshmeh porphyry stock ore sample

3. Sampling and analytical methods

For the present study, 55 large samples (~2-3 kg) were taken from top to bottom of the supergene profile based on sampling from 10 accessible diamond drill-holes, open pit of the mine and waste dumps. Samples divided into three groups (leached, oxidized, enriched) based on core-logging of drill holes, observation of hand specimens, and also microscopic studies on polished and polished-thin sections (Appendix; Table A1). Sample preparation for chemical analysis was done at the SarCheshmeh Copper Complex by using a jaw-crusher for crushing of the samples to particle size 12.7 mm, and followed by grinding in a Cr-steel ring mill to particle size 20 μ m. The samples were analyzed for Cu, Mo, Au, Ag, and also for Fe_2O_3 and SiO_2 at the Central Laboratory of the SarCheshmeh Copper Complex, and in the Chemistry Laboratory of Earth Sciences Development Company, Tehran, Iran. Measurement of Cu, Mo, Fe_2O_3 and SiO_2 was carried out by XRF (with detection limits of 50 ppm for Cu, 10 ppm for Mo, and 0.1 wt% for Fe2O3 and SiO2). Au and Ag were analyzed by Graphite-Furnace Atomic Absorption Spectrometry (detection limit of 0.01 ppm) after pre-concentration by a lead fire assay technique on 25 g sample powder. Analytical data are presented in Appendix (Table A2). Statistically, the data were processed using SPSS.16 software to calculate range and mean values of the metals concentration and also correlation coefficients between the metals in each ore type.

4. Results

The range, mean, and standard deviation for Cu, Mo, Au, Ag concentrations and elemental ratios in supergene ore types are shown in Table 1 and Fig. 4. The Mo abundance in ores ranges between 0.001 wt% and 0.061 wt%. The mean values for Mo in the enriched ores and leached ores are similar, but generally they are higher than those of the oxidized ores (Table 1, Fig. 4). Au concentrations in the supergene ores are generally low, mainly ranging from 0.010 g/t to 0.180 g/t (Table 1, Fig. 5) with one anomalous sample in the enriched ores (0.330 g/t Au). Generally, the highest Au values (from 0.105 g/t to 0.330 g/t) are associated with the enriched ores (Fig. 4). Au abundances are to some extent significantly lower in the leached ores compared to the enriched and oxidized ores (Table 1). The range of Ag values in ores is between 0.42 g/t and 3.85 g/t with anomalous samples from the oxidized and also enriched ores (Table 1, Fig. 4). The mean values for Ag in oxidized ores are higher than other samples (Table 1, Fig. 4). This demonstrates that some Ag is retained in the oxide zone (Table 1). Cu concentrations in ores mainly range between 0.02 and 2.40 wt% with seven anomalous samples in the enriched ores (2.74-5 wt% Cu). Most of the highest Cu values are associated with the enriched ores (Table 1, Fig. 4). In contrast, the leached ores have the lowest Cu values (from 0.02 to 0.09 wt%). The oxidized ores have appreciable Cu values close to main range of the supergene enriched ores (Table 1, Fig. 4). Au/Mo and Cu/Mo ratios are highest in the enriched and oxidized ores where Mo is present in lower abundances but Au and Cu were significantly enriched (Table 1). The Au/Ag ratio in the supergene ores ranges from 0.003 to 0.163;

Oxidized ores have the lowest Au/Ag ratio, whereas the enriched ores show the highest values of Au/Ag ratio. Relationship between the metals in the supergene ore types is shown by the correlation matrices (Table 2). The correlation between elements in ore types shows important discrepancy. In the leached ores, Mo exhibited a moderately positive correlation with Fe_2O_3 (r=+0.75), and is weakly correlated with Cu (r=+0.42) and Ag (r=+0.32). There is no positive correlation between Mo and Au. In these ores, Au is moderately correlated with Ag (r=+0.67) and SiO_2 (r=+0.62). Also, there is a weak positive correlation between Au and Cu (r=+0.31) (Table 2). In the oxidized ores, Mo is negatively correlated with Cu (r=-0.60) as well as with Ag (r=-0.79) (Table 2). Also, there is no positive correlation between Mo and Au (r=+0.08). In these ores, Au is positively correlated with Cu (r=+0.40). There is no clear relationship between Au and Ag (Table 2). Supergene enriched ores show weak positive correlation between Mo and Cu (r=+0.20) as well as between Mo and Au (r =+0.08), with the exception of a strongly positive correlation which exists between Mo and SiO_2 (r=+0.67) (Table 2), whereas there is no significant positive correlation between Au and Cu (r=+0.26). In the enriched ores, there is a moderate positive correlation between Ag and Cu (r=+0.48).

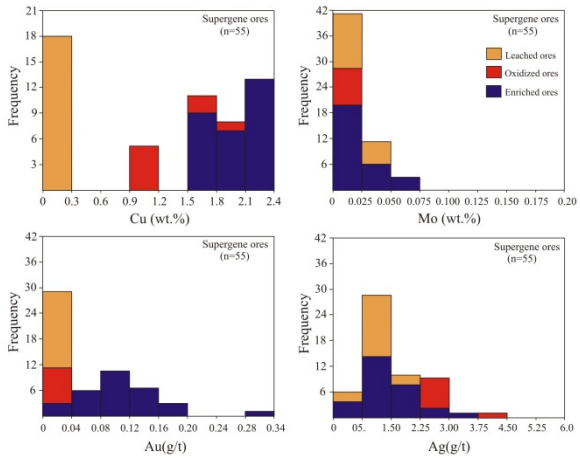

Fig. 4. Comparative histograms of the metal distribution in three types of the supergene ores from the SarCheshmeh deposit

5. Discussion

Trace metals in the supergene profile of the SarCheshmeh deposit show significant differences in distribution pattern and their behavior during supergene enrichment. Bellow, first the metals distribution and relationships between the metals in supergene profile are explained with the supporting mineralogical evidences, then the factors are discussed which control the metal mobility in the supergene profile of the SarCheshmeh deposit.

5.1. Metals distribution

The presence of similar values of Mo in all supergene ore types close to the primary hypogene ores (0.03%; Waterman and Hamilton, 1975; Shafiei and Shahabpour, 2012) indicates that Mo is not significantly depleted from the leached zone and/or enriched in the supergene chalcocite zone. The leached ores with moderately high values of Mo show an approximately high amount of pyrite (see Appendix; Table A1) which can play a critical role for retention of Mo in leached zone. In this regard, the strong positive correlation between Mo and Fe_2O_3 in the leached ores is supported by the presence of ferrimolybdite [$Fe_2(MoO_4)_3.8H_2O$], and also adsorption of Mo by iron hydroxides which is reported by Shahabpour (1991)The weak positive correlation between Mo and Cu in the leached ores may be due to local retention of Cu along with Mo in the leached zone, which could be controlled by the amount of pyrite in primary ores. Similar to Cu, Au has been strongly depleted in the leached zone and significantly enriched in the chalcocite zone. In spite of similar behavior, the weak positive correlation between Au and Cu in the supergene zone could relate to their heterogeneous distribution and also various gold-bearing minerals in the supergene ores. The highest values of Au observed in the enriched ores (0.33 g/t) may be related to the presence of free and visible native gold grains in high-grade Cu ores which were analyzed by Selection Trust (1970) and also indicated by SalariRad et al. (1999) in the SarCheshmeh deposit. Unlike Au, Ag has been partially removed from the leached zone and is locally fixed in the oxidized zone and less in the chalcocite zones. This pattern explains the increasing correlation between Ag and Cu from the leached zone to the oxidized zone. Partial retention of Ag in the leached cap and also the weak positive correlation between Ag and Fe_2O_3 in the leached zone could relate to the presence of arjento-jarosite[$AgFe_3(SO_4)_2(OH)_6$]. Local fixation of Ag in the oxidized zone and strong positive correlation between Ag and Cu in this zone may indicate the presence of Cu and Ag halide minerals such as atacamite [$(Cu_2Cl(OH)_3$] and cerargyrite (AgCl). Although these minerals are not identified in the SarCheshmeh deposit, they are common in the supergene zones that developed in arid to semi-arid and warm climates (Guilbert and Park, 1986). The moderate positive correlation between Ag and Cu in the chalcocite zone could be explained by the possible presence of acantite and argentian chalcocite-group minerals (Sillitoe, 2009).

Table 1. The ranges, means and standard deviations of Mo, Au, Ag, and Cu concentrations and also inter-element ratios in different supergene ore types from the SarCheshmeh deposit

Supergene ores									
	Leached (n=18)			**Oxidized** (n=8)			**Secondary enriched** (n=29)		
	Range	**Mean**	**Stdv.**	**Range**	**Mean**	**Stdv.**	**Range**	**Mean**	**Stdv.**
Cu (%)	0.02-0.09	0.05	0.023	0.89-1.93	1.29	0.409	1.43-5	2.43	0.956
Mo (%)	0.001-0.045	0.020	0.013	0.001-0.017	0.007	0.005	0.004-0.061	0.022	0.016
Au (g/t)	0.010-0.051	0.020	0.009	0.01-0.031	0.021	0.007	0.024-0.330	0.114	0.061
Ag (g/t)	0.42-1.80	1.09	0.348	2.45-3.85	3.07	0.388	0.88-3.20	1.55	0.055
Au/Mo	0.25-20	3.18	0.007	1.61-26	8.56	0.002	1.15-37.5	9.81	0.036
Cu/Mo	0.68-30	5.86	6.47	70-1930	600	640.05	35-1085	223	203.62
Au/Ag	0.009-0.038	0.019	4.652	0.003-0.010	0.007	8.851	0.016-0.163	0.075	8.925

Table 2. Correlation matrices for Mo, Au, Ag, Cu and selected major elements (Fe_2O_3 and SiO_2) in different supergene ore types from the SarCheshmeh deposit. Strong positive correlations are shown in bold.

Ore types		Cu	Mo	Au	Ag	Fe_2O_3	K_2O	SiO_2
Secondary enriched ores	Cu	1						
	Mo	0.20	1					
	Au	0.26	0.08	1				
	Ag	**0.48**	0.05	**0.55**	1			
	Fe_2O_3	-0.21	0.14	-0.12	0.46	1		
	K_2O	**0.61**	-0.04	0.02	-0.42	-0.30	1	
	SiO_2	**0.34**	**0.67**	**0.41**	-0.18	-0.28	0.23	1
Oxidized ores	Cu	1						
	Mo	**-0.60**	1					
	Au	**0.40**	0.08	1				
	Ag	**0.69**	**-0.79**	**-0.28**	1			
	Fe_2O_3	-0.23	**0.19**	0.16	-0.31	1		
	K_2O	0.71	-0.07	-0.07	-0.09	0.23	1	
	SiO_2	-0.59	0.27	**-0.16**	-0.38	-0.31	-0.64	1
Leached ores	Cu	1						
	Mo	**0.42**	1					
	Au	**0.32**	**-0.01**	1				
	Ag	**0.25**	**0.32**	**0.67**	1			
	Fe_2O_3	**0.46**	**0.75**	-0.02	0.29	1		
	K_2O	0.08	-0.18	0.02	-0.01	-0.15	1	
	SiO_2	-0.04	-0.15	**0.62**	**0.47**	-0.21	0.12	1

5.2. Metal mobility

The retention of Mo in the leached zone and significant enrichment of the precious metals together with Cu in the supergene chalcocite zone of the SarCheshmeh deposit indicate that Mo was essentially immobile during supergene oxidation and leaching, whereas the precious metals and Cu are significantly mobile. This emphasizes the different behavior of the metals during supergene processes. Behavior of the metals in the supergene profile could be controlled by local factors such as sulfide mineralogy and alteration type of primary ores as well as climatic influences. These factors control the Eh-pH conditions and metal-transporting capacity of supergene solutions. Restricted mobility and relative enrichment of Mo within the leached ores may be enhanced by leaching of the other constituents from the leached to oxidized zone (Hansuld, 1966; Pokalov and Orlov, 1974). This is confirmed by weak correlations between Mo and other trace metals in the supergene ores. The amount of pyrite in primary ores is one of the most important factors that control Mo mobility in the supergene profile (LeAnderson et al., 1987 and references therein). In phyllitic rocks, where ores have higher pyrite content than those of potassic rocks (Waterman and Hamilton, 1975), Mo could remain within the

leached ores due to strong acidic pH conditions. Under these conditions, the formation of ferrimolybdite prevented leaching of Mo, whereas Cu significantly mobilized and enrichedwithin the supergene chalcocite zone (Fig. 5a, c). In contrast, the pH can remain above the stability field of ferrimolybdite and Mo will be mobile. This took place within ores that have lower pyrite content (ores with high chalcopyrite-pyrite ratio such as potassic ores; Waterman and Hamilton 1975). Where these conditions apply there may be supergene enrichment of Mo in the form of secondary molybdenite such as jordisite and/or castaingite (Brookins, 1988; Fig. 5b). Under these conditions, Cu could be partially retained in the leached cap. These conditions support the inverse relationship between Mo and Cu which is observed in the leached cap. Similar to Cu, the appreciable Au enrichment in the chalcocite zone and also within the oxidized zone not only indicates that most of the Au is transported out of the leached cap under strong acidic conditions, but also this bi-modal enrichment suggests the presence of different ligands for transportation of Au in the supergene profile (Fig. 5a, b, c). Dissolution and transportation of Au during supergene oxidation-leaching process could have mainly occurred in the form of thiosulfate, bisulfide, halide, hydroxyl, or organic complexes (Boyle, 1978; Plyusnin et al., 1981; Stoffregen, 1986; Webster, 1987; Benedetti and Boulegue, 1991; Bowell et al., 1993; Saunders, 1993; Greffie et al., 1996; Cohen and White, 2004; Sillitoe, 2005). The appreciable supergene enrichment of Au suggests the role of auric chloride complexes in further remobilization and dissolution of Au in arid, saline, more acidic and oxidizing solutions (Cloke and Kelly, 1964; Boyle, 1978; Plyusnin et al., 1981; Mann, 1984; Sillitoe, 2005; Fig. 5a). These conditions are consistent with the high pyrite-chalcopyrite ratio in primary ores (e.g., phyllitic ores) and the low neutralizing capacities of these ores. The dry climatic condition for this type of remobilization is predominant in Kerman region, where supergene enrichment zones in some porphyry copper deposits are well developed (Waterman and Hamilton, 1975). The presence of ores with anomalous Au and Ag contents in the leached cap indicate that Au and Ag were not completely removed from the primary ores during supergene oxidation process. This evidence indicates that part of Au and Ag could be essentially inert in iron oxides in leached ores, and no further Au and Ag dissolution would occur. This occurred in pyrite-poor primary ores (i.e., potassic ores), where the relatively weak acidic to near neutral and less oxidizing conditions governs supergene solutions (Fig. 5b). Under these conditions, the thiosulfate complexes are believed to be primarily responsible for local transportation of Au and Ag within the leached cap (Garrels and Thompson, 1960; Boyle, 1978; Nordstorm, 1982; Webster and Mann, 1984; Stoffregen, 1986; Benedetti and Boulegue, 1991; Sillitoe, 2009). Because thiosulfate complexes in relatively acidic environment are readily converted to sulfates (Garrels and Thompson, 1960; Nordstorm, 1982; Stoffregen, 1986), these complexes would rapidly decompose. Consequently, they leave Au and Ag as uncomplexed Au^{+} and Ag^{+} ions (Fig. 5b). They would be precipitated as native Au and Ag with iron and Mn-oxy-hydroxides (Plyusnin et al., 1981; Sillitoe, 2009). This feature is supported by the positive correlation among Au, Ag and Fe_2O_3 in the leached ores, and local increase in Ag content of the leached ores which have moderately high Au contents. This causes a moderate positive correlation between Au and Ag ($r = +0.67$) in these ores. During supergene oxidation process, some parts of Ag would be transported as Ag^{+} in supergene solution (Boyle, 1968). This may be occurr in pyrite-rich ores (Fig. 5a and 5c), where Ag+ mobilized in the highly acidic and oxidizing solution. Under such conditions, Ag precipitated in the oxide zone as arjento-jarosite due to $Fe_2(SO_4)_3$ hydrolysis, and also as native silver (Ag) without gold in the lowermost part of the oxide zone by the reducing action of Fe^{2+}. In these conditions, if Cu is accompaniedby Ag in supergene solution, argentian chalcocite-group minerals may be co-precipitated with acantite in the chalcocite zone (Sillitoe 2009). This support with moderate positive correlation between Ag and Cu in the chalcocite zone may explain the modest supergene enrichment of silver.

6. Conclusions

Study on distribution and geochemical mobility of the trace metals within the supergene profile of the SarCheshmeh porphyry copper deposit indicated that:

1. The precious metals along with Cu significantly depleted in the leached cap and enriched in the oxide and chalcocite zone. In contrast, Mo is partially remained in the leached cap and also shows weak enrichment in the chalcocite zone.
2. The inverse relationship between Mo and Au (and also Cu) distribution in the supergene profile is a function of different mobility of the metals during supergene oxidation-leaching process.
3. The sulfide mineralogy and alteration type of primary ores as well as climatic influences are probably the critical factors controlling mobility of the metals in the supergene profile.
4. Mobility of Mo during supergene oxidation process is likely controlled by the amount of pyrite in primary ores. In primary ores with high pyrite

content, mobility of Mo with formation of ferrimolybdite is greatly restricted. In contrast, in ores with minor pyrite (e.g., SCP ores), Mo could be partially mobilized and enriched in the chalcocite zone.

5. The significant enrichment of Au in the chalcocite zone is thought to be controlled by auric chloride complexes rather than thiosulfate complexes. They are consistent with high acidic supergene solutions which originated from oxidation of highly pyritic ores containing low neutralizing capacity in an arid climate.

6. Although in the supergene profile relatively weak enrichment of Ag along with Cu and Au is recorded in the chalcocite zone, the main part of Ag tends to remain in the oxidized zone.

7. Mobility of Ag as thiosulfate complex in highly acidic and oxidizing solution within the oxide zone could probably be restricted by $Fe_2(SO_4)_3$ hydrolysis and also reducing action of Fe2+(e.g., $Fe^{2+}$of pyrite and chalcopyrite in primary ores). Under such condition, Ag-thiosulfate complex would rapidly decompose and leaved silver as arjento-jarosite and native silver without gold in the lowermost part of the oxide zone.

Acknowledgments

This work was funded by a grant of Golestan University to the author. The author is sincerely grateful to Research and Development Center (R&D) and Mine Affairs of the SarCheshmeh Copper Complex for providing samples, samples preparation, analyses, and also for unpublished new data of the SarCheshmeh deposit.

References

Benedetti, M., & Boulegue, J. (1991). Mechanism of gold transfer and deposition in a supergene environment. *Geochimicaet Cosmochimimica Acta*, 55, 1539–1547.

Brookins, D. G. (1988). Eh-pH diagrams for geochemistry. Springer-Verlag Publication, 175p.

Bowell, R. J., Gize, A. P., & Foster, R. P. (1993). The role of fulvic acid in the supergene migration of gold in tropical rain forest soils. *Geochimicaet Cosmochimica Acta*, 57, 4179–4190.

Boyle, R. W. (1968). The geochemistry of silver and its deposits.*Geological Survey of Canada Bulletin*, 160.

Boyle, R. W. (1978). The geochemistry of gold and its deposits.*Geological Survey of Canada Bulletin*. 280 p.

Chavez, W., & X., Jr. (2000). Supergene oxidation of copper deposits: zoning and distribution of copper oxide minerals. Society of Economic Geology, SEG Newsletter, 41, 12–21.

Cloke, P. L., & Kelly, W. C. (1964).Solubility of gold under inorganic supergene conditions. *Economic Geology*, 59, 259–270.

Cohen, D. R., & White, T. D. (2004). Interaction of aqueous Au species with goethite, smectite and kaolinite. *Geochemical Exploration Analysis*, 4, 279–288.

Etminan, H. (1981). Le porphyrecuprifere de SarCheshmeh (Iran), role des phases fluids dans les mechanisms d'alterationet de mineralization. Geological Survey of Iran, Report, 48, 249p.

Garrels, R. M., & Thompson, M. E. (1960). Oxidation of pyrite by iron sulfate solutions. *American Journal of Science*, 258–A, 57–67.

Greffie, C., Benedetti, M. F., Parron, C., & Amouric, M. (1996). Gold and iron oxide associations under supergene conditions: An experimental approach. *Geochimicaet Cosmochimimica Acta*, 60, 1531–1542.

Guilbert, J. M., & Park, J. C. F. (1986). *The geology of ore deposits*.Freaman and Company, New York, 958p.

Hansuld, J. A. (1966). Behavior of molybdenum in secondary dispersion media.*Society of Mining Engineering, (SME) Transactions*, 73–77.

Haynes, S. J., & Ghorashi-Zadeh, M. (1978). Hydrothermal alteration, Cu mineralization, and supergene pattern, SarCheshmeh, Iran. [Abstract]. Society of Economic Geology, Fall Meeting, Toronto, Canada. *Economic Geology*, 73, 1391–1392.

LeAnderson, P. J., Schrader, E. L., Brake, S., & Kaback, D. S. (1987). Behavior of molybdenum during weathering of the Ceresco Ridge porphyry molybdenite deposit, Climax, Colorado and a comparison with the Hollister deposit, North Carolina. *Applied Geochemistry*, 2, 399–415.

Mann, A. W. (1984). Mobility of gold and silver in lateritic weathering profiles: some observations from Western Australia. *Economic Geology*, 79, 38–49.

McInnes, B. I. A., Evans, N. J., Fu, F. Q., Garwin, S., Belousova, E., Griffin, W. L., Bertens, A., Sukama, D., Permanadewi, S., Andrew, R. L.,&Deckart, K. (2005). *Thermal history analysis of selected Chilean, Indonesian, and Iranian porphyry Cu-Mo-Au deposits*.In T. M. Porter (Ed.), Supper Porphyry Copper and Gold Deposits: A global perspective (pp. 1-16). PGC publishing, Adelaide.

Nedimovic, R. (1973). Exploration for ore deposits in Kerman region. Geological Survey of Iran, Report 53, 247p.

Nordstorm, D. K. (1982). Aqueous pyrite oxidation and formation of secondary iron sulfate and oxide minerals: Acid Sulfate Weathering. *Soil Sciences Society Press*, Madison, Wisconsin, 37–56.

Plyusnin, A. M. Pogrelnyak, Y. F. Mironov, A., & Zhmodik, S. M. (1981). The behavior of gold in the oxidation of gold-bearing sulfides. *Geochemistry International*, 18, 116–123.

Pokalov, V. T., & Orlov, V. G. (1974).Behavior of molybdenum in the oxidation zone. *Geochemistry International*, 11, 447–452.

SalariRad, M. M., Tsunekawa, M., Hirajima, T., & Yoneda, T. (1999). Gold occurrence in the SarCheshmeh porphyry copper ore and its behavior during beneficiation. In: *Proceeding of Copper99, International Environment Conference*, v. II-Mineral Processing/Environment (pp. 129–143).

Saunders, J. A. (1993). Supergene oxidation of bonanza Au-Ag veins at the Sleeper deposit, Nevada, USA: Implications for hydrogeochemical exploration in the

Great basin. *Journal of Geochemical Exploration*, 47, 359–375.

Shafiei, B., & Shahabpour, J. (2012). Geochemical aspects of molybdenum and precious metals distribution in the SarCheshmeh porphyry copper deposit, Iran. *Mineralium Deposita*, 47, 535–543.

Shafiei, B. (2010). Lead isotope signatures of the igneous rocks and porphyry copper deposits from the Kerman Cenozoic magmatic arc (SE Iran), and their magmatic-metallogenetic implications. *Ore Geology Reviews*, 38, 27–36.

Shafiei, B., Haschke, M., & Shahabpour, J. (2009). Recycling of orogenic arc crust triggers porphyry Cu-mineralization in Kerman Cenozoic arc rocks, southeastern Iran. *Mineralium Deposita*, 44, 265–283.

Shahabpour, J. (1982). Aspects of alteration and mineralization at the SarCheshmeh copper-molybdenum deposit, Kerman, Iran. Ph.D. thesis, University of Leeds, England, 342p.

Shahabpour, J., & Kramers, J. D. (1987). Lead isotope data from the SarCheshmeh porphyry copper deposit, Kerman, Iran. *Mineralium Deposita*, 22, 278–281.

Shahabpour, J. (1991). Some secondary ore formation features of the SarCheshmeh porphyry copper-molybdenum deposit, Kerman, Iran. *Mineralium Deposita*, 26, 275–280.

Shahabpour, J. (2000). Behavior of Cu and Mo in the SarCheshmeh porphyry Cu deposit, Kerman, Iran. Can. Institute of Mining and Metallurgy Bulletin, 93, 44–52.

Sillitoe, R. H. (2005). *Supergene oxidized and enriched porphyry copper and related deposits*, In J. W. Hedenquist, J. F. H., Thompson, R. J., Goldfarb, J., Richards, R. (Eds.), 100th Anniversary volume of Economic Geology (pp. 251–298).

Sillitoe, R. H. (2009). Supergene silver enrichment reassessed. In M. S. Enders and S. Titley (Eds.),Supergene Environments, Processes, and Products.*Special Publication of Economic Geology*, 14 (pp. 13–32).

Stoffregen, R. (1986). Observation on the behavior of gold during supergene oxidation at Summitville, Colorado, U.S.A., and implications for electrum stability in the weathering environment. *Applied Geochemistry*, 1, 549–578.

Waterman, G. C., & Hamilton, R. L. (1975). The SarCheshmeh porphyry copper deposit. *Economic Geology*, 70, 568–576.

Webster, J. G. (1987). Thio-sulfate in surficial geothermal waters, North Island, New Zeland. *Applied Geochemstry*, 2, 579–584.

Webster, J. G., & Mann, A. W. (1984).The influence of climate, geomorphology, and primary geology on the supergene migration of gold and silver. *Journal of Geochemical Exploration*, 22, 21–42.

Appendixes

Table A1. Detailed description of 55 supergene ore samples from the SarCheshmeh deposit

Sample No.	Sample location (DDH/ Open pit/Tailing dump)	Host rock	Supergene profile	Alteration and mineralization characters	Ore-type
SC-65	DDH-986;5.5-7m	Andesitic wall-rock	Chalcocite blanket	Disseminated pyrites replaced by chalcocite. Chalcopyrite in a quartz-sericite-chalcopyrite-pyrite replaced by chalcocite.	Enriched ore
SC-66	Open pit	Andesitic wall-rock	Chalcocite blanket	Preferential replacement of chalcopyrite by chalcocite and covelite in crosscutting thin veinlets.	Enriched ore
SC-67	Open pit	Andesitic wall-rock	Chalcocite blanket	Pyrite within the VIII-veinlet partially replaced by chalcocite and covelite.	Enriched ore
SC-68	Open pit	Andesitic wall-rock	Chalcocite blanket	Chalcocite occurs mainly as replacement of chalcopyrite, and to a minor extent as peripheral replacement of pyrite.	Enriched ore
SC-69	Open pit	Andesitic wall-rock	Chalcocite blanket	Covelite replaces both chalcopyrite and chalcocite and to a lesser extent pyrite in VIII-veinlets.	Enriched ore
SC-70	Open pit	Andesitic wall-rock	Chalcocite blanket	Pyrite replaced by chalcocite in a thick quartz-sericite-pyrite±chalcopyrite	Enriched ore
SC-71	Open pit	Andesitic wall-rock	Chalcocite blanket	Chalcopyrite and minor bornite partially or completely replaced by chalcocite and covelite.	Enriched ore
SC-72	DDH-942;70-74m	Andesitic wall-rock	Chalcocite blanket	Disseminated chalcopyrites replaced by chalcocite along their margin.	Enriched ore
SC-73	DDH-987;102-105m	Andesitic wall-rock	Chalcocite blanket	Replacement of pyrite and chalcopyrite (atoll replacement) by chalcocite within a VIII-veinlet.	Enriched ore
SC-74	DDH-987;105-108m	Andesitic wall-rock	Chalcocite blanket	Chalcopyrite and minor pyrite partially replaced by chalcocite and covelite.	Enriched ore
SC-75	Open pit	Andesitic wall-rock	Chalcocite blanket	Replacement of chalcopyrite and pyrite within well-developed crosscutting thin veinlets by chalcocite and covelite	Enriched ore
SC-76	Open pit	Andesitic wall-rock	Chalcocite blanket	Same SC-75	Enriched ore
SC-77	Open pit	Andesitic wall-rock	Chalcocite blanket	Disseminated chalcopyrites/minor pyrite replaced by chalcocite along their margins and fractures.	Enriched ore
SC-78	Open pit	Andesitic wall-rock	Chalcocite blanket	Replacement of chalcopyrite and pyrite by chalcocite and covelite within well-developed crosscutting veinlets which cut a thick quartz-molybdenite veins in a pervasively sericitic sample.	Enriched ore
SC-79	Open pit	Andesitic wall-rock	Chalcocite blanket	Same SC-73	Enriched ore
SC-80	DDH-1002;2.5-7m	SarCheshmeh stock	Chalcocite blanket	Chalcopyrite and pyrite within veinlets partially or completely replaced by chalcocite.	Enriched ore

SC-81	DDH-997;105-106.5m	SarCheshmeh stock	Chalcocite blanket	Relatively thick quartz-molybdenite veins in sample cut by some chalcopyrite/pyrite – bearing veinlets which they replaced by chalcocite and partially by covelite.	Enriched ore
SC-82	DDH-997;106.5-107m	SarCheshmeh stock	Chalcocite blanket	Chalcocite occurs mainly as replacement of chalcopyrite, and to a minor extent as marginal replacement of pyrite.	Enriched ore
SC-83	DDH-997;112-114m	SarCheshmeh stock	Chalcocite blanket	Same SC-81	Enriched ore
SC-84	DDH-997;114-117m	SarCheshmeh stock	Chalcocite blanket	Same SC-81	Enriched ore
SC-85	DDH-1002;150-152m	SarCheshmeh stock	Chalcocite blanket	Same SC-81 with few and thin molybdenite-bearing veinlets	Enriched ore
SC-86	DDH-1002;10-12.5m	SarCheshmeh stock	Chalcocite blanket	Same SC-80	Enriched ore
SC-87	DDH-1003;12.5-13m	SarCheshmeh stock	Chalcocite blanket	Same SC-80	Enriched ore
SC-88	DDH-1002;13-15m	SarCheshmeh stock	Chalcocite blanket	Same SC-80	Enriched ore
SC-89	DDH-1000;13-15m	SarCheshmeh stock	Chalcocite blanket	Same SC-80	Enriched ore
SC-90	DDH-1000;27.5-32.5m	SarCheshmeh stock	Chalcocite blanket	Disseminated relatively coarse chalcocites in a pervasively sericitic-argillic sample. Covelite is also present along the margin of some chalcocites.	Enriched ore
SC-91	DDH-1000;32.5-34.5m	SarCheshmeh stock	Chalcocite blanket	Relatively thick quartz-molybdenite is present. Replacement of chalcopyrite-bornite intergrowth by chalcocite and partially by covelite along its margin	Enriched ore
SC-92	DDH-1000;35-37m	SarCheshmeh stock	Chalcocite blanket	Chalcocite occurs mainly as replacement of chalcopyrites within crosscutting veinlets in a pervasively phyllic sample, and to a minor extent as peripheral replacement of pyrite.	Enriched ore
SC-93	DDH-1000;37-39m	SarCheshmeh stock	Chalcocite blanket	Same SC-91	Enriched ore
SC-94	DDH-1002;0-2.5m	SarCheshmeh stock	Leached cap	The sample pervasively argillized and has yellowish brown color including stains of Fe-oxides and hydroxides	Leached ore
SC-95	Tailing dump	Uncertain	Leached cap	Chalcopyrite and pyrite within veinlets completely replaced by goethite and hematite. Abundant crosscutting quartz-sulfide (Py/Cp) veinlets which partially or completely altered to Fe-oxides and hydroxides.	Leached ore
SC-96	Tailing dump	Uncertain	Leached cap	Colloform texture of hematite and goethite replacing pyrite/chalcopyrite.	Leached ore
SC-97	Tailing dump	Uncertain	Leached cap	Colloform texture of hematite and goethite together with cuprite grains replacing pyrite/chalcopyrite. The sample has some fresh disseminated pyrite	Leached ore
SC-98	Tailing dump	Uncertain	Leached cap	Boxwork texture of hematite and goethite replacing pyrite and chalcopyrite in abundant crosscutting veinlets.	Leached ore
SC-99	Tailing dump	Uncertain	Leached cap	Same SC-95	Leached ore
SC-100	Tailing dump	Uncertain	Leached cap	Partial replacement of chalcopyrite by goethite and hematite within a thick VIII-veinlet. There is some coarse	Leached ore

				pyrite within VIII-veinlets which weakly altered to Fe-oxides and hydroxides.	
SC-101	Tailing dump	Uncertain	Leached cap	Same SC-98	Leached ore
SC-102	Tailing dump	Uncertain	Leached cap	Some pyrite within the VIII-veinlet has been partially altered to Fe-hydroxides. There is a few native-Cu in matrix.	Leached ore
SC-103	Tailing dump	Uncertain	Leached cap	Same SC-100	Leached ore
SC-104	Tailing dump	Uncertain	Leached cap	The sample pervasively argillized and has stains of hematite and goethite. There is abundant pyrite which occurred as crosscutting veinlets.	Leached ore
SC-105	Tailing dump	Uncertain	Leached cap	Abundant crosscutting veinlets including pyrite and a few chalcopyrites which altered to dark brown and yellowish brown of Fe-oxides and hydroxides.	Leached ore
SC-106	DDH-986;0.5-1m	Andesitic wall-rock	Leached cap	Same SC-98	Leached ore
SC-107	DDH-986;1-2.6m	Andesitic wall-rock	Leached cap	Partial replacement of chalcopyrite by goethite and hematite within a thick VIII-veinlet. There is some coarse pyrite as dissemination grains and also within the VIII-veinlet.	Leached ore
SC-108	Tailing dump	Uncertain	Leached cap	Same SC-104	Leached ore
SC-109	Tailing dump	Uncertain	Leached cap	Same SC-105	Leached ore
SC-110	Tailing dump	Uncertain	Leached cap	Same SC-98	Leached ore
SC-111	Tailing dump	Uncertain	Leached cap	Same SC-105	Leached ore
SC-112	Open pit	Andesitic wall-rock	Oxidized zone	The sample has stains of malachite together with hematite/limonite.	Oxidized ore
SC-113	Tailing dump	Uncertain	Oxidized zone	Cuprite grains within fractures including inclusions of native-Cu in a colloform texture of Fe-oxides and hydroxides.	Oxidized ore
SC-114	Open pit	SarCheshmeh stock	Oxidized zone	Spotty green color of secondary copper minerals (probably malachite) within the argillically altered plagioclase phenocrysts.	Oxidized ore
SC-115	Tailing dump	Uncertain	Oxidized zone	Same SC-114	Oxidized ore
SC-116	Open pit	SarCheshmeh stock	Oxidized zone	Same SC-114	Oxidized ore
SC-117	Open pit	Andesitic wall-rock	Oxidized zone	Disseminated native-Cu and cuprite in oxidized and argillized matrix.	Oxidized ore
SC-118	Tailing dump	Uncertain	Oxidized zone	Same SC-117	Oxidized ore
SC-119	Tailing dump	Uncertain	Oxidized zone	Same SC-117	Oxidized ore

Table A2. Analytical data of 55 supergene ore samples from the SarCheshmeh deposit

Sample No.	Cu (%)	Mo (%)	Au (g/t)	Ag (g/t)	Fe_2O_3 (%)	SiO_2 (%)
SC-65	2.20	0.006	0.024	1.45	6.05	53.42
SC-66	2.23	0.018	0.128	2.10	NA	NA
SC-67	1.79	0.017	0.116	1.98	NA	NA
SC-68	2.23	0.016	0.109	1.55	NA	NA
SC-69	2.39	0.017	0.118	2.12	NA	NA
SC-70	1.80	0.019	0.121	1.82	NA	NA
SC-71	2.26	0.018	0.112	1.79	NA	NA
SC-72	1.43	0.005	0.120	1.60	2.85	61.47
SC-73	1.88	0.019	0.150	2	2.97	64.93
SC-74	1.49	0.039	0.062	1.60	3.05	59.52
SC-75	4.34	0.014	0.079	1.60	2.79	59.64
SC-76	4.34	0.004	0.150	1	2.39	74
SC-77	1.48	0.009	0.087	1.10	1.86	56.96
SC-78	5	0.031	0.091	1	0.89	59.71
SC-79	1.82	0.019	0.110	1.75	NA	NA
SC-80	1.60	0.006	0.150	2.67	NA	NA
SC-81	2.11	0.061	0.180	1.30	NA	NA
SC-82	1.81	0.037	0.058	1.20	4.53	71.6
SC-83	2.19	0.058	0.092	1	1.44	76.6
SC-84	2.1	0.055	0.065	1.30	1.86	75
SC-85	2.1	0.029	0.330	3.20	2.39	77.6
SC-86	1.56	0.005	0.130	1.85	0.65	63.39
SC-87	2.10	0.007	0.030	0.88	0.92	64.41
SC-88	1.51	0.004	0.081	1.10	0.64	60.92
SC-89	2.05	0.005	0.048	0.96	0.98	64.47
SC-90	3.86	0.032	0.037	0.88	0.7	77
SC-91	3.63	0.019	0.180	1.20	0.82	72.8
SC-92	2.74	0.032	0.058	1.10	0.78	68.8
SC-93	3.09	0.018	0.180	1.10	0.66	80
SC-94	0.03	0.007	0.051	1.40	7.45	75
SC-95	0.06	0.016	0.015	1.04	18.43	49.13
SC-96	0.02	0.010	0.013	0.52	9.76	46.55
SC-97	0.08	0.020	0.019	1.03	17.33	49.09
SC-98	0.03	0.009	0.016	0.96	15.03	49.87
SC-99	0.06	0.010	0.012	0.78	14.49	47.78
SC-100	0.08	0.020	0.018	0.79	15.73	48.19
SC-101	0.03	0.009	0.016	0.42	10.98	50.06
SC-102	0.08	0.045	0.019	1.40	19.95	48.73
SC-103	0.09	0.021	0.018	1.08	18.11	51.26
SC-104	0.06	0.041	0.023	1.10	19.71	51.65
SC-105	0.07	0.028	0.025	1.45	19.61	52.55
SC-106	0.03	0.001	0.020	1.30	9.81	58.23
SC-107	0.07	0.021	0.030	1.80	9.68	58.64
SC-108	0.03	0.044	0.011	1.16	18.86	48.61
SC-109	0.07	0.012	0.014	0.89	17.09	52.18
SC-110	0.03	0.029	0.010	0.96	17.29	50.04
SC-111	0.07	0.014	0.018	1.48	19.03	48.79
SC-112	1.34	0.017	0.029	2.96	3.86	50.14
SC-113	0.89	0.009	0.023	2.89	4.63	59.66
SC-114	0.91	0.013	0.021	2.45	3.09	63.29
SC-115	0.98	0.007	0.017	3.02	4.18	52.09
SC-116	0.92	0.002	0.010	3.09	3.38	50.18
SC-117	1.38	0.004	0.013	3.17	3.97	49.32
SC-118	1.93	0.001	0.026	3.85	2.55	55.27
SC-119	1.76	0.002	0.031	2.99	4.42	48.09